Rapid Communications

Magnetic field and thermal Hall effect in a pyrochlore U(1) quantum spin liquid

Hyeok-Jun Yang, Hee Seung Kim, and SungBin Lee
Department of Physics, Korea Advanced Institute of Science and Technology, Daejeon 34141, Korea

(Received 12 March 2020; accepted 20 July 2020; published 17 August 2020)

The antiferromagnetic system on a rare-earth pyrochlore has been focused as a strong candidate of U(1) quantum spin liquid. Here, we study the phase transitions driven by external magnetic field and discuss the thermal Hall effect due to emergent spinon excitations with staggered gauge fields. Despite the spinons, the charge excitations of the effective action that carry spin-1/2 quantum number, do not couple to the external field, the emergent U(1) gauge field is influenced in the presence of external magnetic field. In particular, along the [111] and [110] directions, we discuss the possible phase transitions between U(1) spin liquids with different gauge fluxes are stabilized in fields. Beyond the cases where the gauge flux per plaquette is fixed to be either 0 or π, there exists a regime where the staggered gauge fluxes are stabilized without time-reversal symmetry. In such a phase, the thermal Hall conductivity $\kappa_{xy}/T \sim 4.6 \times 10^{-3}$ W/(K^2 m) is expected to be measurable below 1 K.

DOI: 10.1103/PhysRevB.102.060405

Introduction. The exotic phases of matter have broadened the manners to understand the strongly correlated electron systems [1–3]. In particular, quantum spin liquids (QSLs) whose long-ranged order is suppressed even at zero temperature have demanded a new framework to understand internal orders other than the conventional ones [4–6]. One of the fascinating peculiarities of the QSLs is the existence of nonlocal excitations resulting from the quantum entanglement. They characterize the nature of the low-energy excitations which carry fractional quantum numbers. Unfortunately, the experimental probe suffers from the inevitable nonlocality [4,5,7,8]. Nonetheless, several predictions which can be deduced from their low-energy excitations might be an indirect methodology to unveil the phenomena of QSLs.

The rare-earth pyrochlore materials with a chemical formula $R_2TM_2O_7$ contain several candidate materials to realize QSLs [9–21]. Microscopically, the interplay between the highly localized nature of the f electrons in rare-earth ions, strong spin-orbit coupling, and the crystal field results in the effective pseudospin-1/2 model on the pyrochlore lattice [22–27]. Thus, the pseudospin at each site i is represented as $S_i^{\pm}, S_i^z$ about their local $\hat{z}$ axes toward the center of a tetrahedron. Due to the geometrical frustration, the magnetic moment is disordered even at extremely low temperatures. In the absence of quantum fluctuations, the massively degenerate ground states, so-called "two-in two-out" states, are realized [28–31]. In the presence of quantum fluctuations, however, it diagonalizes the ground state manifold to give rise to the fractionalized liquid phase with emergent U(1) gauge structure, dubbed U(1) QSL [32–37].

In this Rapid Communication, we study the U(1) QSLs subject to the external magnetic field uniformly. The U(1) QSLs evolve differently as the field direction changes. We consider two case: the [110] and [111] directions. There is no charge carrier inside the system, thus the degrees of freedom do not couple to the external field through the Peierls substitution. However, the Zeeman coupling with the magnetic dipoles generates the nearest-neighbor spinon hopping. As long as the U(1) QSL persists, i.e., the external field is not too strong, the effective action standing for the emergent gauge field is modified. Importantly, the spinon propagation is coupled to the emergent gauge flux, thus the dynamics of the spinon can be controlled by the external field.

Focusing on the rare-earth pyrochlores described by Kramers doublet for pseudospin (the system contains an odd number of electrons in R^{3+}), we perform the standard perturbation in magnetic field **B** for the lowest-order correction in the coupling constants [33]. Considering the spinon and the associated gauge field, we show there are phase transitions in the U(1) QSL with different fluxes [36,38–40]. We draw the schematic phase diagrams and find the regime where a new type of flux pattern other than the uniform 0 flux (or π flux) are stabilized in every plaquette. When the field is along the [110] direction, 0 and π fluxes coexist and the total flux penetrating the geometrical object enclosed by plaquettes is quantized in units of 2π. However, for the field along the [111] direction, even more complicated flux patterns are manipulated to break the time-reversal symmetry. The emergent Lorentz force then bends the spinon motion, which is reflected in the spinon band structure [41–43]. As a consequence, the thermal Hall effect occurs from the topological spinon bands, $\kappa_{xy}/T \sim 4.6 \times 10^{-3}$ W/(K^2 m) at low temperature below 1 K. We discuss the relevant experiments and generalizations to the other rare-earth pyrochlore materials.

Lattice gauge theory with the Zeeman coupling. We first consider the nearest-neighbor pseudospin-1/2 model on a pyrochlore lattice capturing the essential features of the U(1)

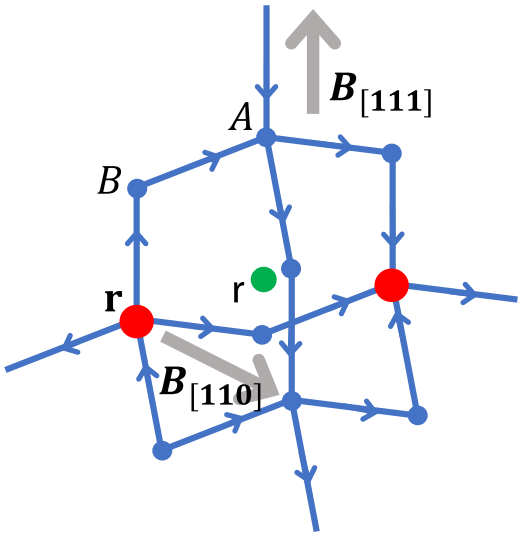

FIG. 1. The diamond lattice with A, B sublattices on which the spinon resides. On the link, the spin degrees of freedom live whose out-of-plane component $S^z_{\mathbf{rr}}$ is marked as a blue arrow. The divergence $\sum_{\mathbf{r}'} S^z_{\mathbf{rr}}$ is identified with the gauge charge density (red circle) at $\mathbf{r}$. The ring exchange is carried out on each of the four hexagonal plaquettes enwrapping the dual diamond site r (green circle) where the magnetic monopole emitting the gauge flux resides. The external B field is applied along the [110] or [111] direction.

QSLs [33].

$$H_{\text{pseu}} = H^z_{\text{pseu}} + H^{\pm}_{\text{pseu}} = \sum_{\langle i,j\rangle} \left\{ J_z S^z_i S^z_j - \frac{J_{\pm}}{2}(S^+_i S^-_j + S^-_i S^+_j) \right\}, \tag{1}$$

where $J_z > 0$ and $J_z \gg |J_{\pm}|$. Here, the pseudospin at each site $S^z_i, S^{\pm}_i$ is defined about their local $\hat{z}$ axis towards the center of a tetrahedron. The first term, Ising interaction, determines the ground state manifold whose elements are called classical spin ice. The classical spin ice infers the spin configurations constrained by the ice rule, two-in-two-out states." Then, the second term serves as a perturbation lifting the degeneracy. The massive amounts of the degeneracy are blended through the quantum tunneling, the second term in Eq. (1).

The second term in Eq. (1) creates a pair of bosonic spinon excitations on the center of the tetrahedra, the diamond lattice [31,44–46]. In Fig. 1, the diamond site is labeled by $\mathbf{r}$ where the pyrochlore site i is located at the center of the diamond bond connecting $\mathbf{r}$ and $\mathbf{r}'$. On the link, the spin variable $S^z_{\mathbf{rr}'}$ can be thought of as an electric field $E_{\mathbf{rr}'} = \epsilon_{\mathbf{rr}'} S^z_{\mathbf{rr}'}$ where $\epsilon_{\mathbf{rr}'} = -\epsilon_{\mathbf{r}'\mathbf{r}} = 1$ when $\mathbf{r} \in A$, $\mathbf{r}' \in B$, and $\epsilon_{\mathbf{rr}'} = 0$ otherwise [33]. Similarly, the in-plane pseudospin $S^+_{\mathbf{rr}'} = \Phi^\dagger_{\mathbf{r}} e^{iA_{\mathbf{rr}'}} \Phi_{\mathbf{r}'}$ induces the spinon $\Phi_{\mathbf{r}}$ to hop from $\mathbf{r}'$ to $\mathbf{r}$ with an emergent U(1) gauge field $A_{\mathbf{rr}'}$ (mod 2π) [33]. These gauge fields satisfy $[A_{\mathbf{rr}'}, E_{\mathbf{rr}'}] = i$ on each link. The exchange interaction in Eq. (1) represents the spinon propagation under the gauge field

$$H_1 = -\sum_{\langle\langle \mathbf{rr}'\rangle\rangle} (t_{\mathbf{rr}'} \Phi^\dagger_{\mathbf{r}} e^{iA_{\mathbf{rr}'}} \Phi_{\mathbf{r}} + \text{H.c.}) - \mu \sum_{\mathbf{r}} \Phi^\dagger_{\mathbf{r}} \Phi_{\mathbf{r}}, \tag{2}$$

where $t_{\mathbf{rr}'} = \frac{J_{\pm}}{2}$ and $A_{\mathbf{rr}'} = A_{\mathbf{rr}''} + A_{\mathbf{r}''\mathbf{r}'}$. For convenience, the spinon charge is set to be $q = 1$ in units of $\hbar = c = 1$. The spinon spectrum is manifest in the band structure Eq. (2) above a finite energy gap $|\mu| \sim J_z$.

By integrating out the gapped spinons in Eq. (2), the third-order perturbation gives the compact U(1) gauge theory with the ring exchange around the hexagonal plaquette [33].

$$H^{(3)}_{\text{eff}} = \frac{U}{2} \sum_{\text{link}} E^2_{\mathbf{rr}'} - \sum_{\text{plaq}} g_p \cos(\nabla \times A_{\mathbf{rr}'}), \tag{3}$$

where $g_p = 3J^3_{\pm}/2J^2_z$ is the coupling constant for the ring exchange. The first term is included to enforce the discreteness of the pseudospin for large $U > 0$ and the second term denotes the lattice curl around the hexagonal plaquette.

In U(1) QSLs, the gapped spinons are deconfined and propagate in the dual lattice. Comparing Eqs. (2) and (3), it is obvious that the gauge flux stabilized by the coupling constant g_p is decisive for the spinon band structure [36,38,40,47]. With unfrustrated $J_{\pm} > 0$, all plaquettes prefer the 0 flux and the spinon band structure is the same as that of the diamond lattice without any gauge field. In the frustrated case $J_{\pm} < 0$, the unit cell is doubly enlarged to stabilize the π flux with the line degeneracy in the band structure [36].

Now we take into account the Zeeman term by applying the external magnetic field $\mathbf{B}$.

$$H_{\text{Zeeman}} = H^z_Z + H^{\pm}_Z = -\sum_i h^z_i S^z_i - \sum_i \left(h^x_i S^x_i + h^y_i S^y_i \right), \tag{4}$$

where the Bohr magneton μ_B and the g factor are absorbed into the definition $h = \mu_B g|\mathbf{B}|$. The subscript i is inserted to remind one that the relative angle between the local axis and the B field depends on four sublattices in a pyrochlore lattice. The spin-flip term in Eq. (4) calls for the nearest-neighbor spinon hopping in Eq. (2), which modifies the coupling constant g_p through the ring exchange. One might expect the gauge flux is always either 0 (or π) for positive (negative) coupling g_p, which preserves the time-reversal symmetry. But this is not the case and we show that the topological bands are stabilized as the field direction $\mathbf{B}$ changes with a moderate strength.

Perturbation of the coupling $\mathbf{g}$ *in fields.* We reinforce our argument in the presence of the B field along the [110] and [111] directions. Since the ring exchange consists of the six subsequent spin flips, the lowest order where h comes in is 4 [48]. When the B field is along the [110] direction, the coupling constants are modified:

$$g^{[110]}_1 = \frac{3J^3_{\pm}}{2J^2_z} + \frac{5J^2_{\pm}h^2}{4J^3_z}, \quad g^{[110]}_2 = \frac{3J^3_{\pm}}{2J^2_z} + \frac{J^2_{\pm}h^2}{J^3_z}, \tag{5}$$

where $g^{[110]}_1$ ($g^{[110]}_2$) is the coupling constant on the plaquette parallel (oblique) to the B-field direction. The difference in the corrections is due to the relative angle between the plaquette and the external B field. When the exchange is unfrustrated ($J^{\pm} > 0$), the B field just enhances the stability of the 0-flux U(1) QSLs. Although higher-order perturbation $\sim h^4 J^2_{\pm}/J^5_z$ may introduce the terms with the opposite signs, it will only renormalize Eq. (5) unless the B field

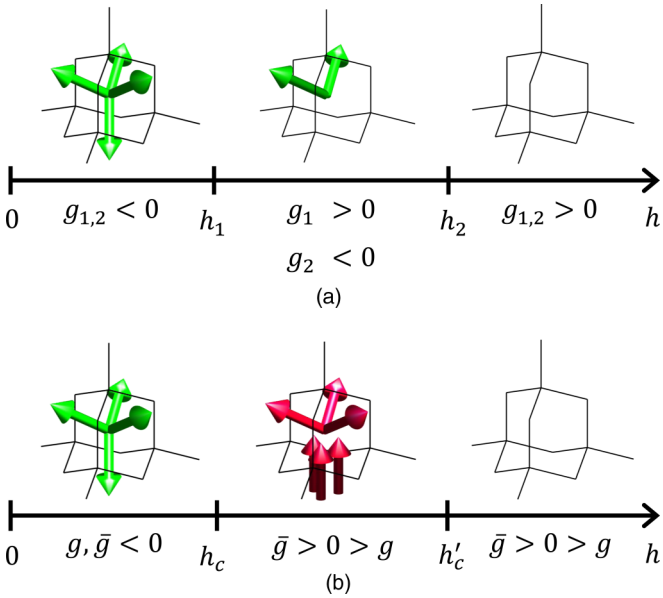

FIG. 2. Schematic phase diagrams with the signs of the coupling constant g_p when the exchange is frustrated $J_\pm < 0$ and the B field is applied along the (a) [110] and (b) [111] directions. The blank, green, and red arrows are identified with 0, π, and continuous $\mathcal{B}$ fluxes, respectively. The phase diagrams are continued until h polarizes the system out of U(1) QSLs.

is relatively large, $h \sim (J_z^3 J_\pm)^{1/4}$. However, in the frustrated case ($J^\pm < 0$), they reverse the coupling constant signs as the B field approaches $h \sim |J_z J_\pm|^{1/2}$ [Fig. 2(a)]. At small field $h < h_1 = 1.10|J_z J_\pm|^{1/2}$, the coupling constants $g_{1(2)}^{[110]}$ are negative implying the π-flux phase. With further increasing $h > h_2 = 1.22|J_z J_\pm|^{1/2}$, all constants in Eq. (5) switch signs and the 0-flux U(1) QSL is stabilized before polarization for large h. In between these two transition points $h_1 < h < h_2$, only two plaquettes among four faces keep the negative constants $g_1^{[110]} > 0$, $g_2^{[110]} < 0$. In this regime, the ground state no longer stabilizes the uniform gauge fluxes. Rather, two 0 fluxes and two π fluxes among four faces are stabilized whose net flux is well quantized. All band structures in three regimes are topologically trivial since the 0 and π fluxes respect the time-reversal symmetry.

Unlike the [110] field case, the field along the [111] direction results in frustrated U(1) gauge fluxes and the nontrivial spinon band structure is stabilized. In this case, the corrections to the coupling constants are [48]

$$g = \frac{3J_\pm^3}{2J_z^2}, \quad \bar{g} = \frac{3J_\pm^3}{2J_z^2} + \frac{10}{9}\frac{J_\pm^2 h^2}{J_z^3}, \tag{6}$$

where the superscript [111] is omitted for convenience. Here, g corresponds to the plaquette perpendicular to the B field and $\bar{g}$ to the other three tilted faces. Similar to the [110] case, the unfrustrated exchange $J_\pm$ is not affected by the applied field. For $J_\pm < 0$, both constants are negative below $h_c = 1.16|J_z J_\pm|^{1/2}$ preferring the uniform π flux. When the B field reaches $h = h_c$, then $\bar{g} = 0$ and the ring exchanges are completely suppressed without the perpendicular kagome plane. At this transition point, the U(1) QSL description fails due to the instanton effect in space-time 2+1 dimension [49].

When $h > h_c$, the phase with staggered flux contains the plaquette preferring the π flux perpendicular to the [111] direction and 0 flux on the others. Thus, one may consider 0 fluxes on three faces and π flux on the other, which is not the case. The obstacle is that the net flux penetrating the four different faces is not quantized in units of 2π. The flux quantization is legitimated by shaving off the preferred flux in each plaquette. Thus we minimize the total magnetic energy instead of each plaquette.

$$\begin{aligned} H_{\text{eff}}^{[111]} &\sim |g|\cos(2\pi - 3\mathcal{B}) - 3\bar{g}\cos(\mathcal{B}) \\ &= 4|g|\cos^3(\mathcal{B}) - 3(|g| + \bar{g})\cos(\mathcal{B}), \end{aligned} \tag{7}$$

where $\mathcal{B}$ is the sheared flux through the three tilted plaquettes. Minimizing Eq. (7), the optimized flux is

$$\left.\frac{dH_{\text{eff}}^{[111]}}{d\mathcal{B}}\right|_{\mathcal{B}=\bar{\mathcal{B}}} = 0, \quad \cos(\bar{\mathcal{B}}) = \sqrt{\frac{|g| + \bar{g}}{4|g|}}. \tag{8}$$

This allows the gauge flux $\mathcal{B}$ other than standard 0 and π fluxes. When h is larger than $h_c' = 2.32(J_z J_\pm)^{1/2}$, then $\bar{g} > 3|g|$ and Eq. (8) has no solution for $\bar{\mathcal{B}}$. In this regime, all plaquettes are enforced to trap the 0 flux, even the negative $g < 0$ one. Between the transition points $h_c < h < h_c'$, the solution $\bar{\mathcal{B}}$ of Eq. (8) is stabilized through the three tilted plaquettes with the $3\bar{\mathcal{B}}$ flux perpendicular plaquette. Here, $\bar{\mathcal{B}}$ is a continuous function of the strength h with the range $0 \leqslant \bar{\mathcal{B}} \leqslant \pi/3$ since $\bar{g} \geqslant 0$.

Staggered flux phase and thermal Hall effect. In the intermediate field $h_c < h < h_c'$ along the [111] direction, the time-reversal symmetry is broken for the generic staggered flux $\bar{\mathcal{B}}$. Since the spinon experiences the emergent gauge flux $\bar{\mathcal{B}}$ (and $3\bar{\mathcal{B}}$), the emergent Lorentz force affects the spinon kinetics [42,43]. This is manifested in the nontrivial spinon band structure with finite Chern numbers. Above the temperature about the spinon gap, this leads to the thermal Hall effect stimulated by the Berry curvature Ω_k [41,50,51]. In this phase, the spinon subject to the magnetic field carries a heat current perpendicular to the temperature gradient.

We numerically evaluate the spinon contribution to the thermal Hall conductivity $\kappa_{xy}(T)$. Nonvanishing coefficient κ_{xy} will signal the relevant evidence for detecting the staggered flux phase. For concreteness, we consider a simple example reasonable for $|J_\pm/J_z| < 1$, $t_{\mathbf{r}\mathbf{r}'} = 1$, and $\mu = -4$ keeping only the nearest-neighbor hopping. We set the gauge field $|g| = \bar{g}$ and $\mathcal{B} = \pi/4$ in Eq. (8). With an appropriate gauge fixing [48], the unit cell of the diamond lattice is enlarged 16 times and the Brillouin zone is folded to yield 32 spinon bands. Based on the band structure, the thermal Hall coefficient $\kappa_{xy}(T)/T$ is evaluated where [51–55]

$$\kappa_{xy}(T) = \frac{k_B^2 T}{\hbar}\sum_{n=1}^{32}\int \frac{d^3k}{(2\pi)^3}\left\{c_2[g(\epsilon_{n,\mathbf{k}})] - \frac{\pi^2}{3}\right\}\Omega_{n,\mathbf{k}}. \tag{9}$$

Here, $\Omega_{n,\mathbf{k}}$ is the Berry curvature at $\mathbf{k}$ on the nth band. The weight $c_2(x) = (1+x)\{\ln[(1+x)/x]\}^2 - (\ln x)^2 - 2\text{Li}_2(-x)$ with a polylogarithmic function $\text{Li}_2(x)$ inherits the role of the Bose distribution $g(\epsilon_{n,\mathbf{k}}) = 1/(e^{\epsilon_{n,\mathbf{k}}/k_B T} - 1)$. Figure 3 shows the thermal Hall conductivity κ_{xy}/T as a function of temperature T. The partially occupied spinon bands give rise to the dominant behavior of κ_{xy}. As the temperature gradually

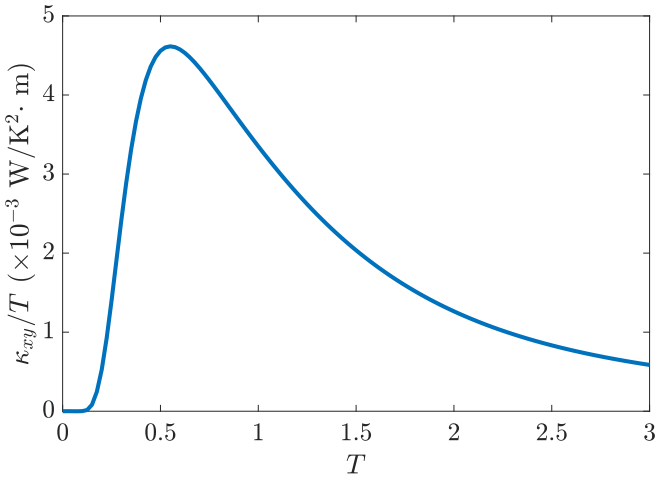

FIG. 3. Numerical plot of the thermal Hall coefficient κ_{xy}/T as the temperature T changes when $|g| = \bar{g}$ and $\bar{\mathcal{B}} = \pi/4$. For simplicity, it is estimated with $t_{\mathbf{rr}'} = 1$ for nearest neighbors only and the chemical potential $\mu = -4$ in Eq. (2). In the vertical axis, the unit is evaluated with respect to the diamond lattice constant ~4.3 Å [46]. In the horizontal axis, the temperature is in units of $t_{\mathbf{rr}'} \sim J_{\pm}$.

increases, it grows from $\kappa_{xy}/T = 0$ towards the peak due to the thermal population. It is noteworthy that the maximum thermal Hall signal reaches $\kappa_{xy}/T \sim 4.6 \times 10^{-3}$ W/(K^2 m) near $T \sim 0.5J_{\pm}$, which is expected to be accessible in experiments [41,56–59]. For further increasing temperature, it vanishes due to the population in the higher bands with opposite signs of the Chern numbers.

Conclusion. We briefly comment on the effect of additional exchange interactions. Despite that our analysis is based on the leading terms Eqs. (1) and (4), it can be generalized to include additional types of exchange interactions. Generically, the symmetry allows other exchanges such as $\sim J_{\pm\pm} S_i^{\pm} S_j^{\pm}/2$ and $\sim J_{\pm z} S_i^{\pm} S_j^{z}/2$ [16,35,36,60]. If the former term $\sim J_{\pm\pm} S_1^{\pm} S_2^{\pm}/2$ is embodied in the ring exchange, the spin at site 1 or 2 is required to be flipped at least three times in succession, thus it does not contribute as a dominant term but plays a role beyond the fourth-order perturbation. Whereas, the latter term $\sim J_{\pm z} S_i^{\pm} S_j^{z}/2$ assembles the Zeeman coupling Eq. (4) and modifies the coupling constants Eqs. (5) and (6) in the same manner. The lowest-order correction [48] results in $\frac{3J_{\pm}^3}{2J_z^2} \to \frac{3J_{\pm}^3}{2J_z^2} + 9\frac{J_{\pm}^2 J_{\pm z}^2}{J_z^3}$ in Eqs. (5) and (6). Likewise the external magnetic field; the frustrated plaquettes $g_p < 0$ reverse their signs at $J_{\pm z} = 0.41|J_{\pm} J_z|^{1/2}$ in the absence of the B field. Thus, below the critical value $J_{\pm z} < 0.41|J_{\pm} J_z|^{1/2}$, the interaction $\sim J_{\pm z} S_i^{\pm} S_j^{z}/2$ induces smaller critical fields in Fig. 2. This enhances the stability of QSLs even turning on B field and one expects the observable κ_{xy} in the regime $h_c < h < h_c' = 2h_c$ where $h_c \to 1.16|J_z J_{\pm} - 6J_{\pm z}^2|^{1/2}$ decreases.

In this Rapid Communication, we study the pyrochlore U(1) QSL applied to the magnetic field. The Zeeman coupling modifies the coupling constant in the emergent U(1) gauge theory, in particular, critically affecting the spinon spectrum. The spinon kinetics experiencing the gauge field is controlled by the strength of the B field. In particular, the preferred fluxes covering the magnetic source are frustrated when the B field is along the [111] direction. This enforces the flux to be shaved off continuously, or even trap the unfavored flux. In this regime, the thermal Hall measurement is an accessible setup to convince the change in emergent gauge structure at low energy. It turns out that spinon bands with frustrated fluxes become topologically nontrivial and result in measurable thermal Hall effect $\kappa_{xy}/T \sim 4.6 \times 10^{-3}$ W/(K^2 m) at low temperature below 1 K. Our argument can be generally applicable to pyrochlore U(1) QSLs, and associated thermal Hall measurement in fields would advocate the U(1) gauge structure and existence of emergent fractional quasiparticles in QSLs. Based on our study, the strain effect in rare-earth pyrochlores with non-Kramers doublet can be another interesting point as relevant future work.

Acknowledgments. We thank Leon Balents, Jeffrey G. Rau, Jung Hoon Han, Gang Chen, Subhro Bhattacharjee, and Nic Shannon for many valuable discussions. This work is supported by the KAIST startup, National Research Foundation Grant No. NRF-2017R1A2B4008097, and in part by the National Science Foundation under Grant No. NSF PHY-1748958.

[1] P. W. Anderson, Mater. Res. Bull. **8**, 153 (1973).
[2] P. W. Anderson, Science **235**, 1196 (1987).
[3] E. Fradkin, *Field Theories of Condensed Matter Physics* (Cambridge University Press, Cambridge, UK, 2013).
[4] L. Balents, Nature (London) **464**, 199 (2010).
[5] L. Savary and L. Balents, Rep. Prog. Phys. **80**, 016502 (2016).
[6] Y. Zhou, K. Kanoda, and T.-K. Ng, Rev. Mod. Phys. **89**, 025003 (2017).
[7] C. Lacroix, P. Mendels, and F. Mila, *Introduction to Frustrated Magnetism: Materials, Experiments, Theory* (Springer Science & Business Media, Berlin, 2011), Vol. 164.
[8] J. C. Wynn, D. A. Bonn, B. W. Gardner, Y.-J. Lin, R. Liang, W. N. Hardy, J. R. Kirtley, and K. A. Moler, Phys. Rev. Lett. **87**, 197002 (2001).
[9] M. J. Harris, S. T. Bramwell, D. F. McMorrow, T. Zeiske, and K. W. Godfrey, Phys. Rev. Lett. **79**, 2554 (1997).
[10] B. Canals and C. Lacroix, Phys. Rev. Lett. **80**, 2933 (1998).
[11] S. T. Bramwell, M. J. Harris, B. C. den Hertog, M. J. P. Gingras, J. S. Gardner, D. F. McMorrow, A. R. Wildes, A. Cornelius, J. D. M. Champion, R. G. Melko, and T. Fennell, Phys. Rev. Lett. **87**, 047205 (2001).
[12] S. Nakatsuji, Y. Machida, Y. Maeno, T. Tayama, T. Sakakibara, J. van Duijn, L. Balicas, J. N. Millican, R. T. Macaluso, and J. Y. Chan, Phys. Rev. Lett. **96**, 087204 (2006).
[13] H. R. Molavian, M. J. P. Gingras, and B. Canals, Phys. Rev. Lett. **98**, 157204 (2007).
[14] J. S. Gardner, M. J. P. Gingras, and J. E. Greedan, Rev. Mod. Phys. **82**, 53 (2010).

[15] J. D. Thompson, P. A. McClarty, H. M. Rønnow, L. P. Regnault, A. Sorge, and M. J. P. Gingras, Phys. Rev. Lett. **106**, 187202 (2011).

[16] K. A. Ross, L. Savary, B. D. Gaulin, and L. Balents, Phys. Rev. X **1**, 021002 (2011).

[17] L.-J. Chang, S. Onoda, Y. Su, Y.-J. Kao, K.-D. Tsuei, Y. Yasui, K. Kakurai, and M. R. Lees, Nat. Commun. **3**, 992 (2012).

[18] K. Kimura, S. Nakatsuji, J. Wen, C. Broholm, M. Stone, E. Nishibori, and H. Sawa, Nat. Commun. **4**, 1934 (2013).

[19] L. Pan, S. K. Kim, A. Ghosh, C. M. Morris, K. A. Ross, E. Kermarrec, B. D. Gaulin, S. Koohpayeh, O. Tchernyshyov, and N. Armitage, Nat. Commun. **5**, 4970 (2014).

[20] L. Pan, N. Laurita, K. A. Ross, B. D. Gaulin, and N. Armitage, Nat. Phys. **12**, 361 (2016).

[21] B. Gao, T. Chen, D. W. Tam, C.-L. Huang, K. Sasmal, D. T. Adroja, F. Ye, H. Cao, G. Sala, M. B. Stone *et al.*, Nat. Phys. **15**, 1052 (2019).

[22] S. Onoda and Y. Tanaka, Phys. Rev. Lett. **105**, 047201 (2010).

[23] S. Onoda and Y. Tanaka, Phys. Rev. B **83**, 094411 (2011).

[24] S. Onoda, J. Phys.: Conf. Ser. **320**, 012065 (2011).

[25] Y.-P. Huang, G. Chen, and M. Hermele, Phys. Rev. Lett. **112**, 167203 (2014).

[26] A. J. Princep, H. C. Walker, D. T. Adroja, D. Prabhakaran, and A. T. Boothroyd, Phys. Rev. B **91**, 224430 (2015).

[27] M. Ruminy, E. Pomjakushina, K. Iida, K. Kamazawa, D. T. Adroja, U. Stuhr, and T. Fennell, Phys. Rev. B **94**, 024430 (2016).

[28] A. P. Ramirez, A. Hayashi, R. J. Cava, R. Siddharthan, and B. Shastry, Nature (London) **399**, 333 (1999).

[29] R. Moessner, Can. J. Phys. **79**, 1283 (2001).

[30] R. Moessner and A. P. Ramirez, Phys. Today **59**, 24 (2006).

[31] C. Castelnovo, R. Moessner, and S. L. Sondhi, Nature (London) **451**, 42 (2008).

[32] R. Moessner and S. L. Sondhi, Phys. Rev. B **68**, 184512 (2003).

[33] M. Hermele, M. P. A. Fisher, and L. Balents, Phys. Rev. B **69**, 064404 (2004).

[34] O. Sikora, F. Pollmann, N. Shannon, K. Penc, and P. Fulde, Phys. Rev. Lett. **103**, 247001 (2009).

[35] L. Savary and L. Balents, Phys. Rev. Lett. **108**, 037202 (2012).

[36] S. B. Lee, S. Onoda, and L. Balents, Phys. Rev. B **86**, 104412 (2012).

[37] N. Shannon, O. Sikora, F. Pollmann, K. Penc, and P. Fulde, Phys. Rev. Lett. **108**, 067204 (2012).

[38] X.-G. Wen, Phys. Rev. B **65**, 165113 (2002).

[39] É. Lantagne-Hurtubise, S. Bhattacharjee, and R. Moessner, Phys. Rev. B **96**, 125145 (2017).

[40] G. Chen, Phys. Rev. B **96**, 085136 (2017).

[41] M. Hirschberger, J. W. Krizan, R. J. Cava, and N. P. Ong, Science **348**, 106 (2015).

[42] Y. H. Gao and G. Chen, SciPostPhysCore **2**, 004 (2020).

[43] X.-T. Zhang, Y. H. Gao, C. Liu, and G. Chen, Phys. Rev. Research **2**, 013066 (2020).

[44] O. I. Motrunich and T. Senthil, Phys. Rev. Lett. **89**, 277004 (2002).

[45] O. I. Motrunich and T. Senthil, Phys. Rev. B **71**, 125102 (2005).

[46] L. D. Jaubert and P. C. Holdsworth, J. Phys.: Condens. Matter **23**, 164222 (2011).

[47] A. M. Essin and M. Hermele, Phys. Rev. B **87**, 104406 (2013).

[48] See Supplemental Material at http://link.aps.org/supplemental/10.1103/PhysRevB.102.060405 for details on the local coordinates conventions, the magnetic coupling constants Eqs. (5) and (6), gauge fixing with a flux $\bar{\mathcal{B}} = \pi/4$ in Eq. (8), and its spinon band spectrum, which includes Refs. [16,33,35,36].

[49] A. M. Polyakov, Phys. Lett. B **59**, 79 (1975).

[50] H. Katsura, N. Nagaosa, and P. A. Lee, Phys. Rev. Lett. **104**, 066403 (2010).

[51] S. Murakami and A. Okamoto, J. Phys. Soc. Jpn. **86**, 011010 (2016).

[52] J. Luttinger, Phys. Rev. **135**, A1505 (1964).

[53] L. Smrcka and P. Streda, J. Phys. C: Solid State Phys. **10**, 2153 (1977).

[54] R. Matsumoto and S. Murakami, Phys. Rev. Lett. **106**, 197202 (2011).

[55] R. Matsumoto, R. Shindou, and S. Murakami, Phys. Rev. B **89**, 054420 (2014).

[56] M. Hirschberger, R. Chisnell, Y. S. Lee, and N. P. Ong, Phys. Rev. Lett. **115**, 106603 (2015).

[57] Y. Kasahara, T. Ohnishi, Y. Mizukami, O. Tanaka, S. Ma, K. Sugii, N. Kurita, H. Tanaka, J. Nasu, Y. Motome *et al.*, Nature (London) **559**, 227 (2018).

[58] Y. J. Yu, Y. Xu, K. J. Ran, J. M. Ni, Y. Y. Huang, J. H. Wang, J. S. Wen, and S. Y. Li, Phys. Rev. Lett. **120**, 067202 (2018).

[59] M. Hirschberger, P. Czajka, S. Koohpayeh, W. Wang, and N. P. Ong, arXiv:1903.00595.

[60] Z. Hao, A. G. R. Day, and M. J. P. Gingras, Phys. Rev. B **90**, 214430 (2014).